# Chapter 4

# Gaussian Optics

In the following chapter, an overview of the theory of Gaussian optics will be given to the extent needed to describe the resonator and transmission line of the spectrometer. To a great extent, this treatment will follow those of (P. F. Goldsmith 1998) and (Kogelnik & Li 1966).

## 4.1 Gaussian Beams

To derive a formula that describes the propagation of a beam of microwave radiation along the $z$–axis, we begin with the Helmholtz wave equation for a uniform medium:

$$\left(\nabla^2 + k^2\right)\psi = 0 \tag{4.1}$$

Here, $\psi$ represents any component $\mathbf{E}$ or $\mathbf{B}$ of the radiation field and $k = 2\pi/\lambda$ is the propagation constant in the medium.

Since we want to describe a beam traveling in $z$–direction, we assume a functional form of the field components of

$$\psi(x, y, z) = u(x, y, z)\exp(-ikz) \tag{4.2}$$

where the non–plane–wave behavior is described by $u$. Inserting this into equation 4.1 we arrive at the reduced wave equation:

$$\frac{\partial^2 u}{\partial x^2} + \frac{\partial^2 u}{\partial y^2} + \frac{\partial^2 u}{\partial z^2} - 2ik\frac{\partial u}{\partial z} = 0 \tag{4.3}$$

The third term can be dropped under the paraxial approximation, which states that the variation of $u$ along the $z$–direction is small compared to the variation in $x$ and $y$ and in particular that it will be small over a distance of the order of one wavelength. This then leads to the paraxial wave equation

$$\frac{\partial^2 u}{\partial x^2} + \frac{\partial^2 u}{\partial y^2} - 2ik\frac{\partial u}{\partial z} = 0 \tag{4.4}$$

In cylindrical coordinates with $r^2 = x^2 + y^2$, the reduced wave equation becomes

$$\frac{\partial^2 u}{\partial r^2} + \frac{1}{r}\frac{\partial u}{\partial r} + \frac{1}{r}\frac{\partial^2 u}{\partial \varphi^2} - 2ik\frac{\partial u}{\partial z} = 0 \tag{4.5}$$

where the angular dependency on $\varphi$ can be dropped under the assumption of cylindrical symmetry to yield the axially symmetric paraxial wave equation:

$$\frac{\partial^2 u}{\partial r^2} + \frac{1}{r}\frac{\partial u}{\partial r} - 2ik\frac{\partial u}{\partial z} = 0 \tag{4.6}$$

This equation has solutions of the form:

$$u(r, z) = \frac{\omega_0}{\omega}\exp\left[\frac{-r^2}{\omega^2} - \frac{i\pi r^2}{\lambda R} + i\phi_0\right] \tag{4.7}$$

where

$$\omega = \omega_0\sqrt{1 + \left(\frac{\lambda z}{\pi\omega_0^2}\right)^2} \tag{4.8}$$

$$R = z + \frac{1}{z}\left(\frac{\pi\omega_0^2}{\lambda}\right)^2 \tag{4.9}$$

$$\tan\phi_0 = \frac{\lambda z}{\pi\omega_0^2} \tag{4.10}$$

Equation 4.7 describes a diverging beam with a minimum diameter at $z = 0$. $\omega$ is the distance from the beam axis where the amplitude has reached $1/e$

times that on the axis. The quantity $\omega_0$ is the so–called beam waist — the $\omega$–radius of the beam at its minimum diameter. $R$ can be identified as the radius of curvature of the phase front where it intersects the $z$–axis.

This can also be seen from the exponent in equation 4.7 where the first term leads to the Gaussian beam profile perpendicular to the axis and the second resembles an outgoing spherical wave.

From equation 4.2 follows the expression for the complex field:

$$\psi(r,z) = \frac{\omega_0}{\omega} \exp\left[\frac{-r^2}{\omega^2} - ikz - \frac{i\pi r^2}{\lambda R} + i\phi_0\right] \tag{4.11}$$

For calculations of coupling of Gaussian beams it is helpful to normalize the beams to unit power flow, by requiring the integral over the beam area to be unity:

$$\int_0^\infty |\psi|^2 \, 2\pi r \, dr = 1 \tag{4.12}$$

This leads to a different prefactor in equation 4.11, so that the normalized fundamental Gaussian beam mode becomes

$$\psi(r,z) = \sqrt{\frac{2}{\pi\omega^2}} \exp\left[\frac{-r^2}{\omega^2} - ikz - \frac{i\pi r^2}{\lambda R} + i\phi_0\right] \tag{4.13}$$

The analogous result for a Gaussian beam with uniform distribution in $y$–direction will be needed in the calculation of beam overlap in section 4.3 and can be derived in a corresponding treatment to the one above:

$$\psi(x,z) = \sqrt[4]{\frac{2}{\pi\omega_x^2}} \exp\left[\frac{-x^2}{\omega_x^2} - ikz - \frac{i\pi x^2}{\lambda R_x} + \frac{i\phi_{0x}}{2}\right] \tag{4.14}$$

It is helpful to introduce a further parameter, the confocal distance $z_c$:

$$z_c = \frac{\pi\omega_0^2}{\lambda} \tag{4.15}$$

It can be seen as the distance separating the "near field" and "far field" regions of the Gaussian beam. The radius of curvature of the Gaussian

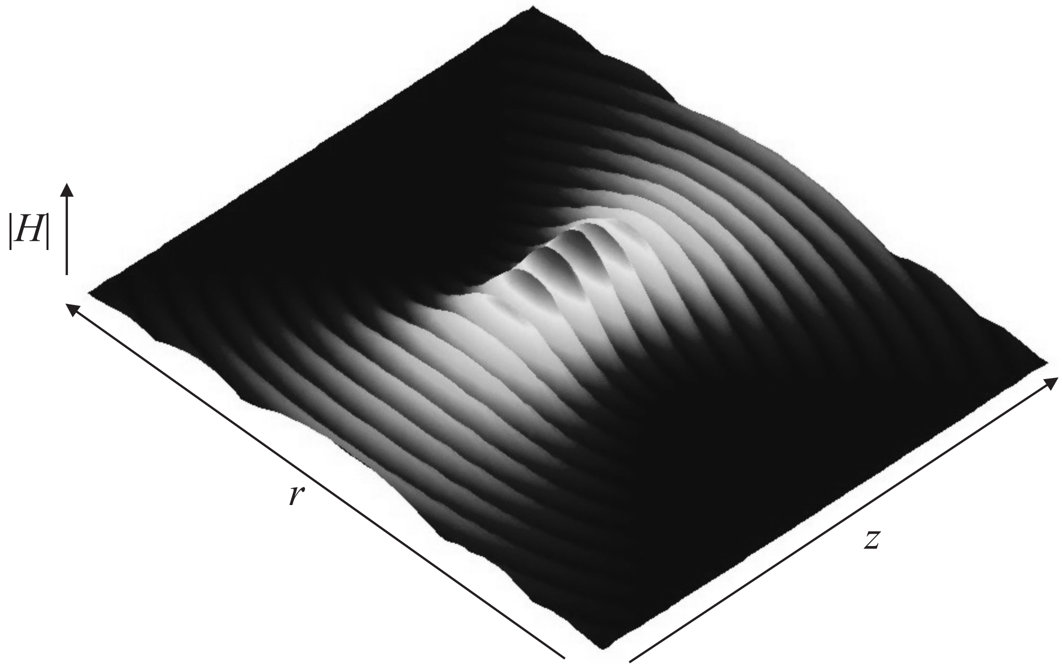


Figure 4.1: Amplitude profile of a Gaussian beam. Note the Gaussian intensity profile in $r$–direction and the (nearly) spherical phase fronts.

beam $R$ has a minimum at a distance $z = z_c$ away from the beam waist at $z = 0$.

The parameters describing the Gaussian beam can then be rewritten in a more compact form as:

$$\omega = \omega_0 \sqrt{1 + \left(\frac{z}{z_c}\right)^2} \tag{4.16}$$

$$\phi_0 = \arctan\left(\frac{z}{z_c}\right) \tag{4.17}$$

$$R = z\left(1 + \left(\frac{z_c}{z}\right)^2\right) \tag{4.18}$$

In the far field, equation 4.16 can be used to derive an expression for the asymptotic beam growth angle $\theta_0$:

$$\theta_0 = \lim_{z>>z_c} \left[\arctan\left(\frac{\omega}{z}\right)\right] = \arctan\left(\frac{\lambda}{\pi\omega_0}\right) \tag{4.19}$$

where usually the small angle approximation can be applied, so $\theta_0 \cong \lambda/\pi\omega_0$. So the beam in the far field grows linearly with the distance from the beam waist.

The general solution of the wave equation 4.1 in cylindrical coordinates includes higher order modes that allow for variation in the angular coordinate $\varphi$ and deviate from the Gaussian intensity profile of the fundamental mode.

The complete result for the normalized Gaussian beam mode in cylindrical coordinates shall just be quoted here:

$$\begin{aligned}\psi_{pm}(r,\varphi,z) &= \sqrt{\frac{2p!}{\pi(p+m)!}}\,\frac{1}{\omega(z)}\left[\frac{\sqrt{2}r}{\omega(z)}\right]^m L_{pm}\left(\frac{2r^2}{\omega^2(z)}\right)\\ &\quad\cdot\exp\left[\frac{-r^2}{\omega^2(z)} - ikz - \frac{i\pi r^2}{\lambda R(z)} - i(2p+m+1)\phi_0(z)\right]\\ &\quad\cdot\exp(im\varphi)\end{aligned} \tag{4.20}$$

$L_{pm}$ is the generalized Laguerre polynomial with the radial index $p$ and the angular index $m$. The modes are normalized in terms of the normalization condition of equation 4.12

## 4.2 Modes in the Fabry–Perot Resonator

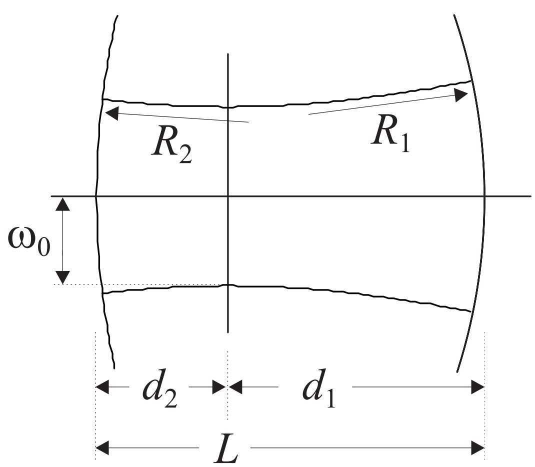


Figure 4.2: Fabry–Perot resonator: general non–symmetric configuration. Beam waist $\omega_0$, waist to mirror distances $d_1$, $d_2$, radii of curvature $R_1$, $R_2$, mirror to mirror distance $L$

To obtain the mode pattern in a Fabry–Perot resonator, the resonator can be unfolded into an equivalent infinite sequence of lenses. The resonance condition then becomes the requirement that all parameters of the Gaussian beam become the same after passing one full period of the lens sequence, or after one complete round trip between the two mirrors, respectively.

From the transformation laws for the lenses then follows a condition that allows one to determine the resonant beam waist $\omega_0$ in dependence of the resonator parameters $f_1$, $f_2$ and $L$ as depicted in figure 4.2. The focal lengths $f_i$ of the mirrors can be obtained from the radius of curvature of the mirrors, where $f_i = R_i/2$.

For a symmetric resonator with $f_1 = f_2 = f$ and $d_1 = d_2 = d$, this leads to an expression for the confocal distance:

$$\begin{aligned} z_c &= \frac{L}{2}\sqrt{\frac{4f}{L} - 1} \\ &= d\sqrt{\frac{R}{d} - 1} \end{aligned} \tag{4.21}$$

from which the beam waist in the resonator can be calculated:

$$\omega_0^2 = \frac{\lambda d}{\pi}\sqrt{\frac{R}{d} - 1} \tag{4.22}$$

In our case we have a half–symmetric resonator with a plane mirror at the position of the symmetry plane of the symmetric mirror, so $L = 2d$ has to be replaced by $L = d$. The beam waist in this configuration obviously lies on the plane mirror.

We now want to determine the mirror distances $d$ at which we can observe resonant behavior. This can be translated into the condition that the phase of the Gaussian beam of equation 4.7 must be a multiple of $2\pi$ after one complete round trip through the resonator. The phase shift of an axially symmetric Gaussian–Laguerre beam (equation 4.20) relative to its beam waist is

$$\phi_{pm}(z) = -i\left(kz - (2p + m + 1)\,\phi_0\right) \tag{4.23}$$

with $\phi_0$ given by equation 4.17. The resonance condition for the general resonator

$$\Delta\phi = 2\left[\frac{2\pi L}{\lambda} - \left(\arctan\left(\frac{d_1}{z_c}\right) + \arctan\left(\frac{d_2}{z_c}\right)\right)\right] = 2\pi q \qquad (4.24)$$

becomes for the case of a symmetric mirror ($d_1 = d_2 = d$):

$$2kd - 2\,(2p + m + 1)\arctan\left(\frac{d}{z_c}\right) - q\pi = 0 \qquad (4.25)$$

with $q$ the number of half-wavelengths and $p = m = 0$ for the fundamental mode. This can then be solved numerically for the resonant mirror separation $d$.

This result implies that the higher modes have different resonance frequencies from the fundamental mode, with the exception of the case of the exactly confocal configuration with $d = z_c$. The resonator should therefore be operated in a near confocal mode, while avoiding the exact confocal configuration.

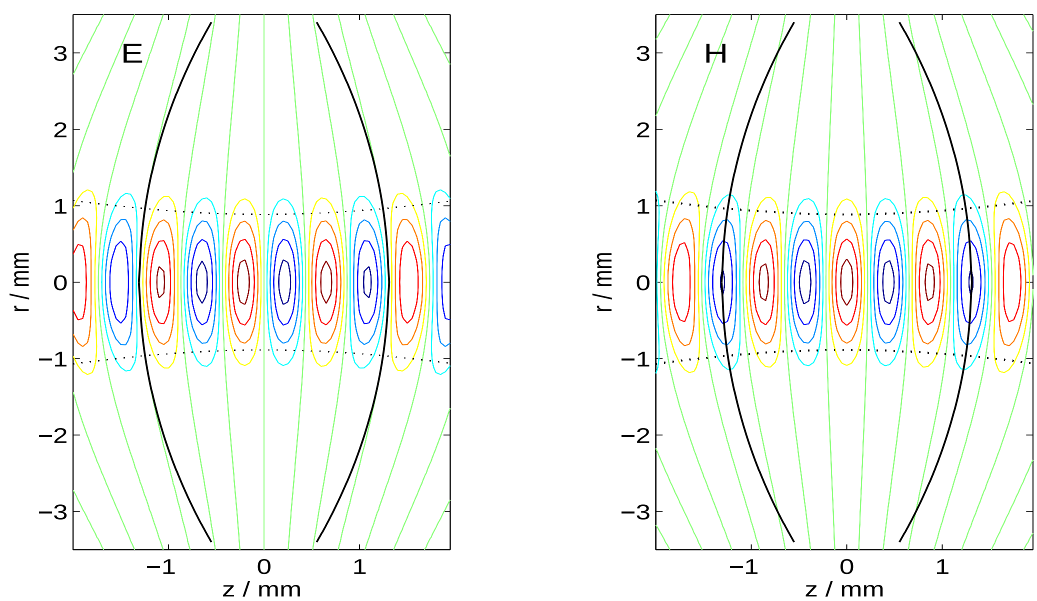


Figure 4.3: Contour plots of a $\mathrm{TEM}_{006}$ mode in a symmetric Fabry–Perot resonator. The left picture shows the electric, the right picture the magnetic field amplitude. The resonator dimensions are: $R = 8.06$ mm, $d = 1.3$ mm.

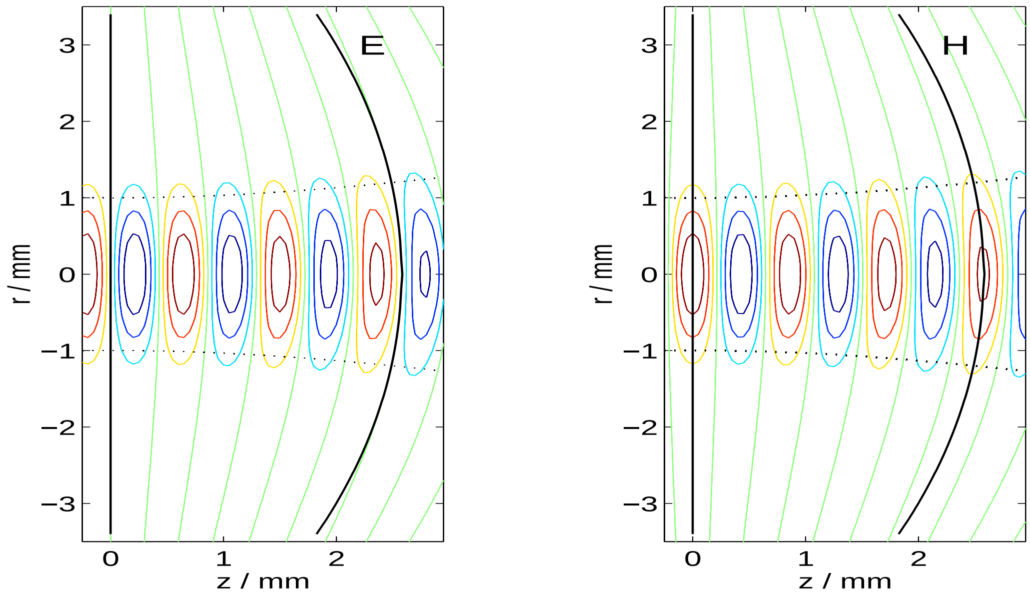


Figure 4.4: Contour plots of a $TEM_{006}$ mode in a half-symmetric Fabry–Perot resonator. The left picture shows the electric, the right picture the magnetic field amplitude. The dimensions are identical to the actual resonator in the spectrometer: $R = 8.06$ mm, $d = 2.6$ mm.

It is important to note here that the Gaussian beam that is determined by the above parameters $(\omega_0, z_c)$ is only an approximation to the actual modes in the resonator, since the curvature of the phase fronts deviates considerably from the spherical shape of the mirrors for larger values of $r$, as can be clearly seen in the contour plots in figure 4.4. Since for our EPR experiment we are mainly interested in the size of the area of maximum field, the approximation of the modes with a Gaussian beam is sufficiently accurate, however.

## 4.3 Coupling of Gaussian Beams

An central issue in designing and setting up a Gaussian beam transfer line is the sensitivity of the system to misalignment. Since in our case, the microwave setup does not consist of one single piece, it has to be realigned frequently. It is therefore of importance to know which kind of misalignment results in the most serious insertion loss and how critical it is.

In the following, coupling efficiencies for various types of misalignment will be derived (P. F. Goldsmith 1998).

The general problem is that of two Gaussian beams that shall be made to overlap perfectly (couple). An example would be a beam being focussed by a mirror onto a detector antenna. The second beam in this example is the characteristic component beam of the antenna, the beam that would emanate from it were it a source– instead of a detector–antenna.

In principle there are three different kinds of misalignment:

- If both beams share the same optical axis, but their beam radii $\omega$ or radii of curvature $R$ are mismatched, they are the so–called axially aligned beams. Here, only the special case of two beams with equal but longitudinally displaced beam waist $\omega_0$ will be considered, since this corresponds to the situation encountered in the spectrometer microwave bridge.
- The optical axis of both beams can be laterally displaced.
- The optical axes of both beams can be tilted with respect to each other.

To obtain an expression that allows us to calculate power losses due to imperfect coupling, we start with the field coupling coefficient of two Gaussian beams:

$$c_{ab} = \int\int \psi_a^* \psi_b \, dS \tag{4.26}$$

This is often written in "bra–ket" notation as:

$$c_{ab} = \langle \psi_a | \, \psi_b \rangle \tag{4.27}$$

The integral usually is taken over a plane perpendicular to the optical axis, the so–called reference plane. In case of coinciding beam waists, the reference plane will be placed there.

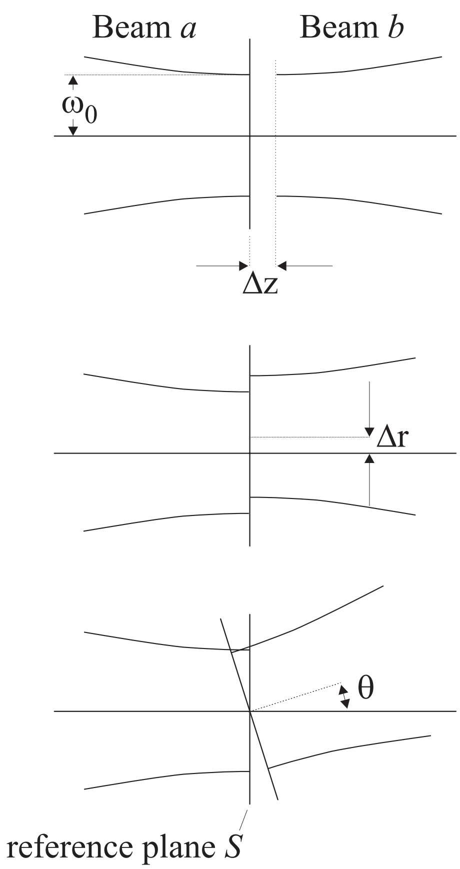


Figure 4.5: Gaussian beam coupling for misaligned beams: Longitudinally displaced beams (top), laterally displaced beams (middle), tilted beams (bottom)

Since we are interested only in power transmission, the overall phase terms can be ignored, so using equation 4.2, equation 4.26 becomes:

$$c_{ab} = \int\int u_a^* u_b \, dS \tag{4.28}$$

If evaluated in the $x$ coordinate only, it is denoted

$$c_{ab}^{1x} = \int\int u_a^*(x) u_b(x) \, dx \tag{4.29}$$

and the two dimensional field coupling coefficient $c_{ab}^2$ is then obtained by:

$$c_{ab}^2 = c_{ab}^{1x} \, c_{ab}^{1y} \tag{4.30}$$

Separating the Cartesian coordinates will prove useful when considering the different kinds of misalignment.

The fraction of the power actually being coupled from beam $a$ into beam $b$ is given by the power coupling coefficient $K_{ab}$, the square of the field coupling coefficient

$$K_{ab} = \left|c_{ab}^2\right|^2 \tag{4.31}$$

This expression can now be evaluated for the different situations depicted in figure 4.5:

Assuming that the two beams to be coupled are axially aligned, have cylindrical symmetry around the optical axis and have the same beam waist, one can obtain the field coupling coefficient for longitudinal displacement $c_{\text{long}}^2$ by inserting equation 4.14 into equation 4.28 and squaring:

$$c_{\text{long}}^2 = \frac{\exp\left(-ik\Delta z\right)}{1 - i\lambda\Delta z/2\pi\omega_0^2} \tag{4.32}$$

and, by squaring the absolute value, the power coupling coefficient:

$$K_{\text{long}} = \left|c_{\text{long}}^2\right|^2 = \frac{4}{4 + \left(\lambda\Delta z/\pi\omega_0^2\right)^2} \tag{4.33}$$

$\Delta z$ is the distance between the beam waists $\omega_0$ along the axis as shown in figure 4.5 (top).

A similar procedure, considering a lateral offset in $x$ direction by $\Delta r$ yields the lateral power coupling coefficient

$$K_{\text{lat}} = \exp\left(-\frac{\Delta r^2}{\omega_0^2}\right) \tag{4.34}$$

This simple expression only holds for equal and coinciding beam waists, however.

In the case of angular misalignment (assuming a tilt angle $\theta$ in $x$–direction), the phase of beam $b$ is shifted with respect to beam $a$ by $\Delta\phi = -kx\sin\theta$ when moving a distance $x$ along the $x$–axis. Assuming no longitudinal or lateral displacements, the angular power coupling coefficient can be obtained as:

$$K_{\mathrm{ang}} = \exp\left(-\left[\frac{\pi\theta\omega_0}{\lambda}\right]^2\right) \tag{4.35}$$

The approximation for small angles $\theta$ was used in the derivation.

### Estimation of coupling efficiency

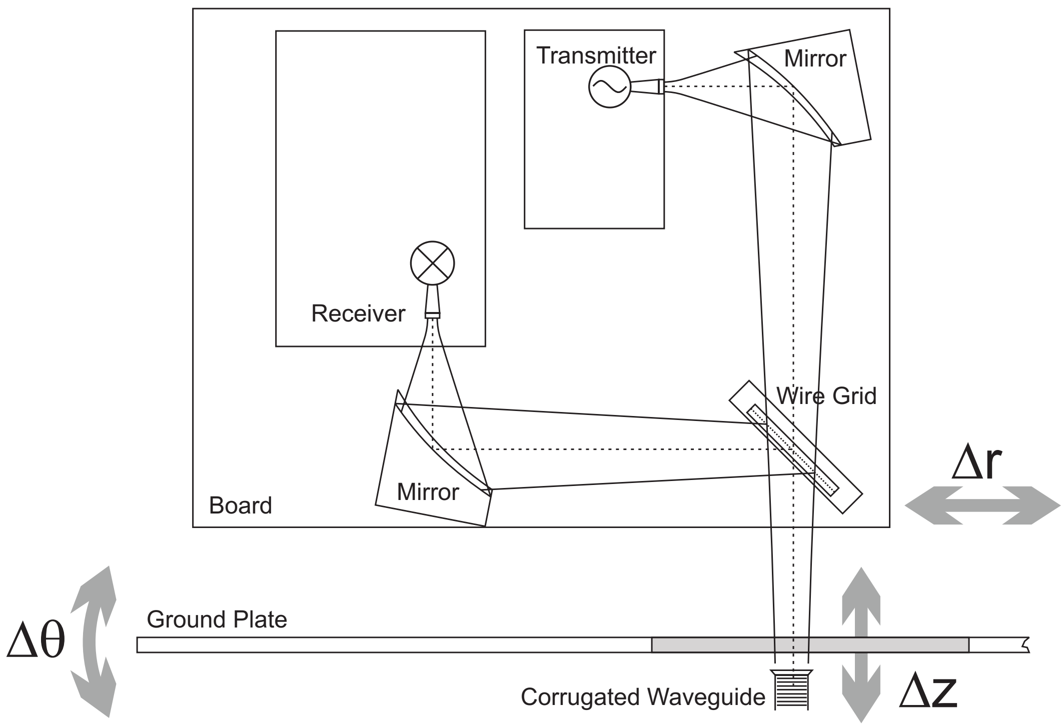


Figure 4.6: Quasi optical setup on the optical board and degrees of freedom for alignment of the board with respect to the corrugated waveguide in the magnet bore.

The expressions derived above allow one to estimate how critical each alignment parameter $(\Delta z, \Delta r, \theta)$ is at various places in the quasi optical transfer line. Of particular importance for the alignment process are the beam waists at the transmitter antenna and at the upper end of the corrugated waveguide at the top of the magnet (see figure 4.6). Since the transfer line components on the optical board are mounted completely independently from the corrugated waveguide in the magnet bore, especially the alignment at the waveguide entrance is of interest.

The maximum deviations for each parameter that correspond to power losses of 1% and 10% respectively are listed in table 4.1, table 4.2 and table 4.3.

| Maximum $\Delta z$ | Tx | WG |
|---|---|---|
| $K_{long} > 0.9$ | 16.5 mm | 131.8 mm |
| $K_{long} > 0.99$ | 5.5 mm | 39.5 mm |

Table 4.1: Maximum longitudinal displacement $\Delta z$ for coupling losses under 10% and 1% at the transmitter antenna (Tx, $\omega_0 = 1.48$ mm) and the corrugated waveguide entrance (WG, $\omega_0 = 7.24$ mm).

| Maximum $\Delta r$ | Tx | WG |
|---|---|---|
| $K_{lat} > 0.9$ | 0.48 mm | 2.35 mm |
| $K_{lat} > 0.99$ | 0.15 mm | 0.73 mm |

Table 4.2: Maximum lateral displacement $\Delta r$ (all other conditions are identical to table 4.1).

| Maximum $\theta$ | Tx | WG |
|---|---|---|
| $K_{ang} > 0.9$ | 3.33 ° | 0.68 ° |
| $K_{ang} > 0.99$ | 1.03 ° | 0.21 ° |

Table 4.3: Maximum angular misalignment $\theta$ (all other conditions are identical to table 4.1).

It becomes clear that longitudinal deviations are uncritical; also lateral offsets should readily be met. Angular deviations, on the other hand, prove to be extremely critical if insertion losses at the transmitter antenna and especially at the waveguide entrance are to be minimized. This is of even greater importance since alignment at the waveguide involves the adjustment of the complete optical board.

The result that a small beam waist is less sensitive to angular misalignments at first seems counterintuitive, but can be related to the inverse dependence of the beam growth angle on the beam waist (equation 4.19). Less divergent beams are more sensitive to angular deviations of the optical axis.